MODELING AND EVALUATING TRAFFIC FLOW AT SAG CURVES WHEN IMPOSING VARIABLE SPEED LIMITS ON CONNECTED VEHICLES

Reza Vatani Nezafat
rvata001@odu.edu

Ehsan Beheshtitabar
ebehe001@odu.edu

Mecit Cetin
mcetin@odu.edu

Old Dominion University
Department of Civil & Environmental Engineering

135 Kaufman Hall
Norfolk, Virginia 23529-0001 USA
757-683-3753
Fax 757-683-5354

Elizabeth Williams
egwilli4@ncsu.edu

George F. List
gflist@ncsu.edu

North Carolina State University
Department of Civil, Construction, and Environmental Engineering

208 Mann Hall
2501 Stinson Drive, Campus Box 7908
Raleigh, NC 27695-7908 USA
209-681-3422
Fax 919-515-7908

Submission Date: August 1, 2017
Word count: 5354 + (8*250) = 7,354

ABSTRACT

Sag curves, road segments where gradient changes from downwards to upwards, generally reduce the roadway capacity and cause congestion. This results from the change in longitudinal driving behavior when entering a sag curve as drivers tend to reduce speeds or increase headways as vehicles reach the uphill section. In this research, a control strategy is investigated through manipulating the speed of connected vehicles (CVs) in the upstream of the sag curve to avoid the formation of bottlenecks caused by the change in driver behavior. Traffic flow along a sag curve is simulated using the intelligent driver model (IDM), a time-continuous car-following model. A feedback control algorithm is developed for adjusting the approach speeds of CVs so that the throughput of the sag curve is maximized. Depending on the traffic density at the sag curve, adjustments are made for the speeds of the CVs. A simulation-based optimization method using a meta-heuristic algorithm is employed to determine the critical control parameters. Various market penetration rates for CVs are also considered in the simulations. Even at relatively low market penetration rates (e.g., 5-10 %), significant improvements in travel times and throughput are observed.

INTRODUCTION

Motivated by their major safety and mobility impacts, connected vehicles (CVs) equipped with two-way wireless communications capabilities are expected to be widely available in the near future. Some automakers are already installing Dedicated Short Range Communication (DSRC) devices in their new vehicles that allow the exchange of vehicle-to-vehicle (V2V) and infrastructure-to-vehicle (I2V or V2I) information. Given the expected availability of I2V or V2V communications with increasingly more vehicles in the traffic stream, it is important to study how various types of traditional infrastructure-centric traffic flow control methods would operate in a CV environment. For example, I2V communication technologies could be a replacement for the dissemination of information through variable message signs. This paper's main focus is to investigate how potential implementation of variable speed limit (VSL) through CVs could impact traffic flow. To illustrate such impacts, a VSL algorithm is implemented in a simulation environment to control the inflow to a sag curve on a freeway to minimize delays and increase throughput.

The simulation environment consists of three building blocks (I) a longitudinal driving behavior model describing car-following dynamics; (II) a proportional feedback control law for setting VSLs in the upstream; (III) a framework for optimization of model parameters. An essential element of the first component pertains to the characterization of driving behavior of vehicles in the sag curve, especially as they climb the uphill. For this purpose, a recent car-following model developed in 2016 by Goñi-Ros *et al.* incorporates the impacts of gradient on vehicle acceleration is adapted *(1)*. Using the Intelligent Driver Model (IDM) as the basis, the model by Goñi-Ros *et al.* adjusts a vehicle's acceleration on the uphill by accounting for how much or how quickly the driver can compensate for the influence of the grade resistance force in reducing vehicle speed. Details of this are presented later in the paper. Similar to the control law implemented in Goñi-Ros *et al*., an ALINEA proportional feedback control law is applied to the second component *(2, 3)*. For the last component of the simulation environment, a meta-heuristic algorithm is developed to find the optimum model parameters.

LITERATURE REVIEW/BACKGROUND

Traffic dynamics are generally recreated in a simulation environment by categorizing vehicle behavior into longitudinal and lateral components. Longitudinal behavior fundamentally corresponds to the acceleration of a vehicle while lateral behavior to choosing and changing lanes. In this study, the lateral behavior will not be considered because the investigated network contains a single-lane freeway.

The fundamental macroscopic relationship between traffic flow, density, and speed depends on the characteristics of longitudinal driving behavior. Empirical observations show that vehicles move at the free flow speed when density is low. As density increases, they maintain free flow speed until it reaches a certain critical density point. Beyond this point, further increases in density would result in lower speeds, and consequently lower traffic flow. Capacity is then defined as the maximum flow reached at the critical density. Researchers have noted that capacity of congested traffic conditions is significantly lower than that of free flow traffic conditions, and the magnitude of the drop is dependent on traffic flow and relative speeds *(4-6)*. This difference is called the capacity drop phenomena. Daganzo explained that bottlenecks arise at sections with abrupt increases of demand such as on-ramps or at tunnels and weaving sections where capacity would drop suddenly *(7)*. Based on the Transportation Research Board's (TRB) fifth edition of the Highway Capacity Manual, transient events such as weather conditions or accidents can also cause a local drop in the capacity of freeways leading to bottlenecks *(8)*. In hilly regions, sag curves are one of the most common causes of bottlenecks. Researchers, such as Okamura in 2000 and Xing in 2010, have shown that the capacity of a sag curve is 10 to 25 percent lower than level sections *(9, 10)*. Later in 2014, Xing *et al.* have noted that sag curves are the main reason behind 60 percent of bottlenecks on Japanese intercity freeways *(11)*.

A sag curve is defined as a downhill followed by an uphill or as a section where the gradient of roadway increases gradually in the direction of traffic. Previous studies showed that drivers reduce their desired speeds at sags *(12, 13)*. In 2012, Yoshizawa *et al.* suggested that the main reason of this reduction is related to poor acceleration behaviors on sags *(14)*. However, Laval *et al.* put forward that when power to mass ratio is considerably large, the reason may be related to insufficient acceleration capability of drivers *(15)*.

Many researchers have developed microscopic mathematical models to reproduce the characteristics of traffic flow at sags. These car-following models are designed to take into account the influence of gradient on vehicle acceleration *(16, 17)*. Yoshizawa *et al.* noticed that when drivers reach a sag curve, they cannot fully compensate for the increase in the slope *(14)*. Other studies have added compensation for the limiting effect which increases in gradient has on vehicle acceleration *(18, 19)*. Empirical observations have shown that models which consider compensation for drivers can reproduce longitudinal driving behavior and traffic dynamics at sag curves more accurately. More recently, in 2012, Goni-Ros *et al.* introduced another term in the acceleration equation of the Intelligent Driver Model (IDM) to incorporate this effect of compensation for driving behavior *(1, 20)*. The developed model can capture the effect of compensation on a vertical curve. They have assumed drivers would compensate the gradient linearly along the sags in the direction of uphill.

There are several active traffic management (ATM) strategies for reducing congestion at sags, such as queue warning and Variable Speed Limits (VSL). Some field tests and simulation experiments have been conducted to evaluate the effectiveness of these approaches. The goals of these strategies are increasing the capacity of sags, preventing the formation of congestion at

sags, and increasing the queue discharge capacity of sags. For instance, the capacity of sag could be increased by utilizing adaptive cruise control systems to perform the acceleration task more efficiently than humans *(21)*. Another study proposed to inform the location of the queue's head to drivers at upstream to encourage them to speed up after leaving congestion *(22)*. One of the most popular ATM strategies is variable speed limits (VSLs). For instance, Goni-Ros *et al*. evaluated the possibility of maximizing the throughput of a sag bottleneck by implementing VSL at the upstream of the bottleneck through a variable message sign*(2)*. It was assumed that all drivers would comply with the VSL, which generally is not a realistic assumption. In this paper, the VSL is imposed only on the CVs, for which the market penetration is varied from zero to 100 percent. Therefore, the results of this paper could also be used to analyze the impacts of compliance rate on the system performance.

The control strategy used in this study is inspired by one of the most popular ramp-metering algorithms called ALINEA *(3)*. However, the parameters of this algorithm have to be calibrated to achieve the maximum system efficiency. To do so, one common technique is to employ meta-heuristics, such as a Genetic Algorithm (GA), which are used in various models *(23)*. Genetic algorithms are very popular and easy to use, but they have slow convergence and are weak in the local search *(24)*. Another meta-heuristics method, Particle Swarm Optimization (PSO), is very suitable for complex continuous problems because of its simplicity due to having few parameters. Despite its advantages, PSO usually fails to control its velocity step size for better tuning in search space, resulting in inappropriate results *(25)*. Many researchers use a combination of these algorithms to overcome the drawbacks of each. This study uses an algorithm called HPSOGA which is a combination of Genetic Algorithm (GA) and Particle Swarm Optimization (PSO) proposed by Duan *et al.* in 2013 *(26)*. It captures the advantages of both algorithms and converges faster.

LONGITUDINAL DRIVING BEHAVIOR

In this study, the model Goni-Ros *et al*. proposed for sag curves is used *(1)*.This model accounts for the influence of vertical curves on vehicle acceleration. It calculates acceleration from the summation of two terms as presented in Equation 1. The first component corresponds to car-following behavior and the second one calculates behavior on uphill.

$$\upsilon'(t) = fr(t) + fg(t) \quad (1)$$

The first acceleration term uses speed (v), relative speed (Δv), the desired speed (υ_{des}), and spacing to the vehicle ahead (s) to calculate acceleration for the following car. This is a modified version of the IDM.

$$fr(t) = a \times \min\left[1 - \left(\frac{\upsilon(t)}{\upsilon_{des}}\right)^4, 1 - \left(\frac{s_{des}(\upsilon(t), \Delta\upsilon(t))}{s(t)}\right)^2\right] \quad (2)$$

In Equation 2, s_{des} is the desired spacing which is computed using Equation 3. The main influencing factor is the safe gap to the lead vehicle.

$$s_{des}\big(\upsilon(t), \Delta\upsilon(t)\big) = s_0 + \upsilon(\mathrm{t}).\tau\big(\upsilon(\mathrm{t})\big) + \frac{\upsilon(\mathrm{t}).\Delta\upsilon(\mathrm{t})}{2\sqrt{a.b}} \quad (3)$$

The a is the maximum acceleration, b is the maximum comfortable deceleration, s_0 is the gap at the standstill situation, and τ is the safe time headway as a function of speed. Based on the traffic state, the safe time headway (τ) changes as shown in Equation 4.

$$\tau(\upsilon(t)) = \begin{cases} \tau_f & \upsilon(t) \geq \upsilon_{crit} \\ \gamma.\tau_f & \upsilon(t) < \upsilon_{crit} \end{cases} \quad (4)$$

The second term ($fg(t)$) in Equation 1 captures the influence of gradient on vehicle acceleration. This influence is equal to the difference between the gradient at the position of the vehicle ($G(x(t))$) and the compensated gradient by the driver at the time ($G_c(t)$) multiplied by gravity acceleration. This is shown in Equation 5.

$$fg(t) = -g.(G(x(t)) - G_c(t)) \quad (5)$$

Ros *et al*. assumed that drivers would compensate linearly for any increase in freeway gradient with maximum gradient compensation rate defined by parameter c.

$$G_c(t) = \begin{cases} G(x(t)) & G(x(t)) \leq G(t_c) + c(t - t_c) \\ G(t_c) + c(t - t_c) & otherwise \end{cases} \quad (6)$$

Where:

$$t_c = \max\left[t \mid G_c(t) = G(x(t))\right] \quad (7)$$

If the increase in grade over time is lower than c, then $G_c(t)$ is equal to $G(x(t))$ and $fg(t)$ is zero. Hence, the acceleration of vehicle is not affected and the driver fully compensates for the gradient.

CONTROL STRATEGY

The objective of the control strategy is to eliminate congestion in sags and improve the performance of highways in hilly regions. For networks not influenced by other control measures, minimizing the total time that vehicles spend in the system is equivalent to maximizing the exit flow *(27)*. As mentioned previously, under uncongested traffic conditions, flow or throughput is higher than that under congested conditions. The capacity of the freeway on a sag section (q_{Sag}) is less than other sections ($q_{Capacity}$). Therefore, the network's exit flow is limited by the capacity of the sag bottleneck.

$$q_{Exit} \approx q_{Sag} < q_{Capacity} \quad (8)$$

One way to maximize the exit flow is to prevent traffic from becoming congested at the bottleneck. Keeping traffic state uncongested at the bottleneck is possible if the inflow of the sag gets regulated at a controlled section at the upstream. The inflow of sag is approximately equal to the outflow of the control section, and per the fundamental relation between speed and flow, changing speed on control section changes the inflow of the sag. By dynamically modifying the speed at control section, it is possible to keep the inflow to the bottleneck slightly below its free flow capacity. This will increase the time-weighted sum of exit flow. When the demand in the upstream is large enough, the congestion would not be prevented completely. As a result, the control section and upstream would become congested instead of the sag curve, but the outflow from the controlled part will be higher than the queue discharge capacity of the sag.

The controller which calculates speed limit for the control section is inspired by the ramp-metering control algorithm called ALINEA and proposed by Papageorgiou *et al*. *(3)*. This algorithm is based on the basics of a proportional feedback control law. It calculates the variable speed limit based on Equation 9. The target density (ρ_{Target}) is slightly lower than the critical density of fundamental diagram, and real-time density (ρ_b) is the estimated density at the sag curve calculated every T_c seconds. The algorithm would change the speed limit as a proportion

(κ) of the difference between target and measured density every time that a new density is calculated.

$$\upsilon_{Limit}(t) = \upsilon_{Target} + \kappa \times (\rho_{Target} - \rho_b(t-1)) \qquad (9)$$

As evident from Equation 9, in high demand conditions, the controller would keep the density at bottleneck close to target density to prevent breakdown. Whenever demand decreases, the measured density would be significantly less than target density which leads the controller to impose a higher speed limit and, in contrary, if demand increases measured density would be substantially more than target density which leads the controller to enforce a lower speed limit. The controller always uses the previously estimated density so that drivers would have enough time to cover the distance between the control section and the bottleneck.

Two roadside units, shown in Figure 1, are needed for system operation. The roadside unit A is connected to a typical loop detector that measures occupancy and estimates density at the bottleneck every T_c seconds. This information is then transmitted to roadside unit B in the upstream. Based on Equation 9, the roadside unit B would update speed limit every T_c seconds and broadcast it to the connected vehicles (CVs) when they arrive at the control section every second. The geometry of the network and traffic flow parameters are explained next.

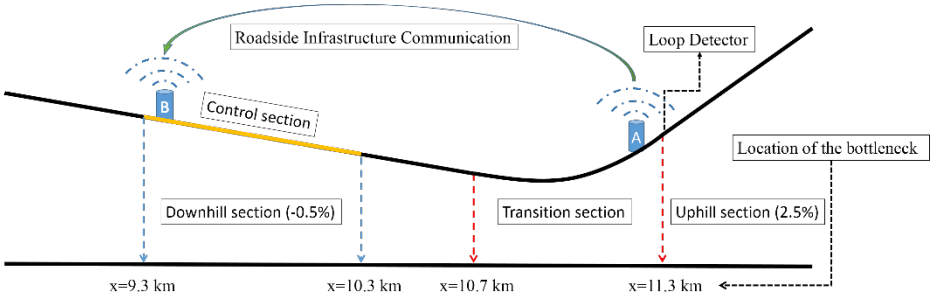

FIGURE 1 Geometry of the sag curve

SIMULATION SETUP

The simulation model comprises a one-lane freeway with a sag in the middle. The length of the facility is 12 km. The road starts with constant-gradient downhill section followed by a vertical sag curve, and at the end, a constant-gradient uphill section (see Figure 1). The downhill section has a constant gradient equal to -0.5 percent and the uphill section has a constant slope equal to 2.5 percent. At the vertical sag, the slope increases linearly from -0.5 to +2.5 percent, and the length of the vertical curve is 400 m between x = 10.7 km and x = 11.3 km. The downhill section is long enough to make sure queue would not reach the entry point of the simulation. The speed limit is 120 km/h. Characteristics of vehicles and drivers, as defined by the IDM model, are assumed to be homogeneous to prevent the emergence of other types of bottlenecks in the simulation. These model parameters are shown in Table 1.

TABLE 1 Characteristics of the car-following model

$\upsilon_{des}(km/h)$	$a(m/s^2)$	$b(m/s^2)$	$\tau(s)$	$s_0(m)$	$\upsilon_{crit}(km/h)$	$\gamma(-)$	$c(s^{-1})$	$\Delta t(s)$
120	1.45	2.1	1.2	3	65	1.15	0.0001	0.5

The distribution of demand over time is illustrated in Figure 2. The first 10 minutes is a transition from zero to 2400 veh/h, a capacity higher than the bottleneck capacity. The demand

stays at 2400 veh/h for 30 minutes then transitions back to zero across 10 minutes. Beyond this, the demand remains zero until all vehicles have exited the facility.

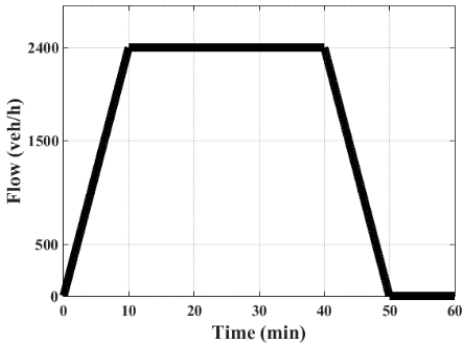

FIGURE 2 Demand profile over time

The control section in Figure 1 is 1.0 km long. In this section, only connected vehicles would be informed of the calculated speed limit. Notably, it is assumed that all CVs would comply completely. The control section is between x = 9.3 km and x = 10.3 km. The downstream end of the controlled section is 0.4 km away from the beginning of the transition section. As soon as connected vehicles leave the control section, their speed will revert to the default 120 km/h to make sure the vehicles traverse the uphill with the maximum speed possible. In other words, the desired speed of CVs is only varied while they are within the control section.

With the given parameters above, a microsimulation model was created in MATLAB. In Figure 3, a heatmap along with sample vehicle trajectories are shown (middle chart) for the base case, i.e. when no control strategy is implemented. At the very beginning of the simulation, the effect of the uphill is not significant enough to cause a breakdown at the bottleneck. After a while, a shockwave starts to propagate backward starting at the bottleneck with constant speed. Since the breakdown is due to the geometry of the road, this shockwave continues to propagate until in-flow decreases.

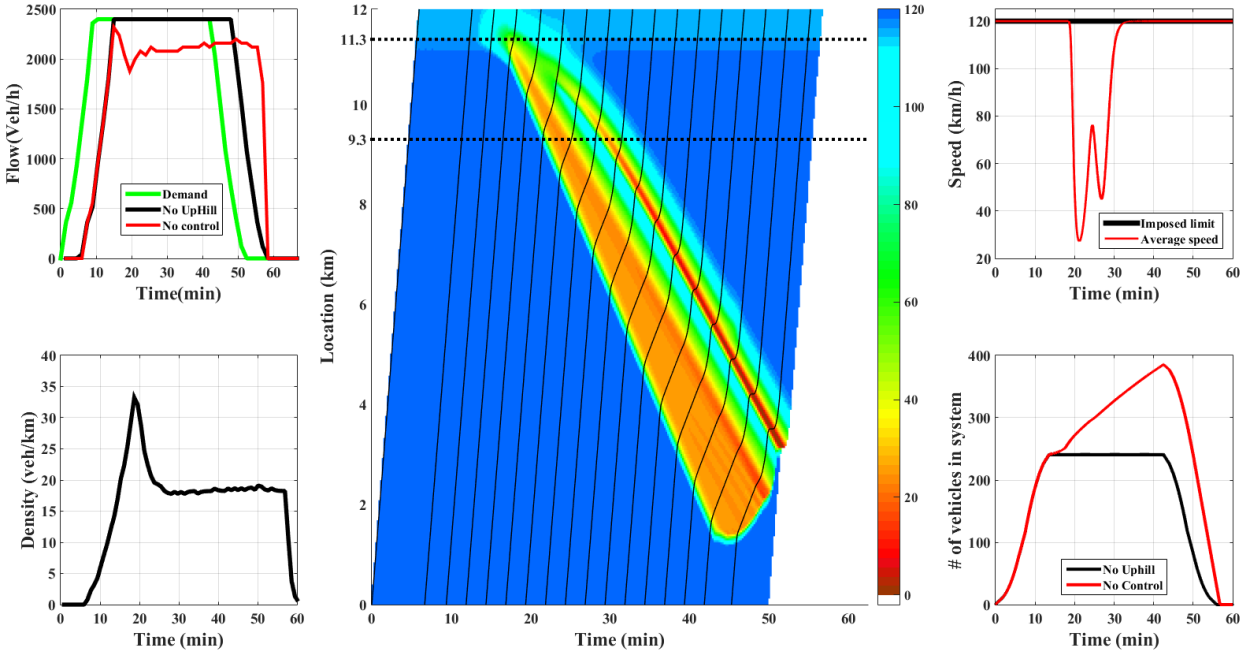

FIGURE 3 Input demand and exit flows (top left), density measured by loop detector (bottom left), heat-map with sample trajectories (middle), average vehicle speeds in the control section (top right), and number of vehicles in the system (bottom right) without a VSL control system

Four other charts are included in Figure 3 to provide additional performance measures for analysis. At the top left, the input demand over time (green line), as well as exit flow rates, are depicted for the base case (red line). A hypothetical scenario (black line) where the uphill has no influence whatsoever on the traffic flow is also shown. This last scenario is included as a reference to show the maximum possible system performance if the effects of sag are eliminated. This phenomenon could perhaps be achieved through automated driving, but this is left for future research. The second chart, density versus time plot at the lower left, shows the measured density by the loop detector at the uphill (see Figure 1). The chart on the top right shows the observed speed (red line) at the control section as well as the imposed VSL. The last chart at the bottom right reports the total number of vehicles in the system, i.e. for the entire corridor, over time for the base case without a VSL system (red line) as well as for the hypothetical scenario (black line). These charts are reproduced to summarize the effects of VSL under various CV market penetrations as presented later in the paper.

A META-HEURISTIC FOR THE OPTIMAL CONTROL PARAMETER VALUES

The VSL control strategy described by Equation 9 requires three key parameters to achieve optimal performance. Here, the total delay in the system is used as the objective function. The delay for a vehicle is computed in reference to the hypothetical scenario mentioned above, where the sag curve is assumed to have no influence on the traffic flow. For the simulated demand, vehicles travel through the corridor at free flow speeds. For a given scenario, the total delay is the sum of the individual vehicle delays. For example, when there is no VSL control system, the system performs as shown in Figure 3. This total delay (TD) is then taken as a reference and compared to the total delay for theVSL control strategies. Consequently, the objective function is defined as shown in Equation 10.

$$ObjectiveFunction = \frac{TD_{NoControl} - TD_{Controlled}}{TD_{NoControl}} \quad (10)$$

Optimizing three parameter values is the objective: the gain (κ), the period for sampling occupancy at bottleneck (T_c), and the target speed (υ_{Target}). Since a mathematical formulation for this optimization problem does not exist, the authors used a meta-heuristic. The hybrid particle swarm optimization genetic algorithm (HPSOGA) proposed by Duan *et al. (26)* was employed.

The particle swarm optimization (PSO) simulates the behavior of a swarm of particles moving to a potential well with an analogy to the flocking of birds or fish schooling. Random parameters for all particles are generated and the objective function for each particle is calculated. For this problem, a good position for a particle corresponds to a lower value of the objective function. The particles move in the search space of the problem to find the lowest value of the objective function. The particles are guided by their own best known experience in the search-space as well as the entire population's best experience. Each iteration best experiences get updated both individually and globally.

The solution from the PSO becomes the initial population of the genetic algorithm. The genetic algorithm (GA) has three stages: Stage 1: Creating an initial population; Stage 2: Evaluating an objective function; and Stage 3: Producing a new population. GA operators

manipulate each member. The first operator is a crossover which selects two members of the population as parents and produces two offspring by swapping elements of the parents. Participating in a crossover depends on the value of each member's objective function which means members with higher values participate in crossovers more often. The second operator is a mutation operator. It is used to increase the space explored. The mutation rate is low. In the end, a new population is selected from the output of these two operators and the process continues. If identical solutions are obtained, the best solution is assumed to be determined.

The three control parameters were optimized using HPSOGA algorithm with a population size of 50 and a maximum iteration number of 100. The optimal parameters found by the algorithm are presented below:

- Target speed, $v_{Target} = 95\ (km/h)$
- Gain, $\kappa = 4.68$
- Updating period, $T_c = 50\ (s)$

The resulting system performance is shown in Figure 4. The market penetration rate is 100%. The VSL reduced the total delay by 49% compared to the no control scenario. The shockwave is moved upstream of the control section. The density at the bottleneck stays below 25 veh/km at the onset of congestion and the system is able to reach a steady-state density and approximately constant VSLs after 35 minutes. In the top-right chart, it is clear that vehicles adhere to the imposed VSLs since their average speeds follow the VSLs. In the bottom-right graph, the blue-line approximately splits the area between black and red lines into two equal pieces, visually demonstrating that the total delay is reduced by about 50%. It should also be noted that the queue dissipation time is shorter under the VSL control system.

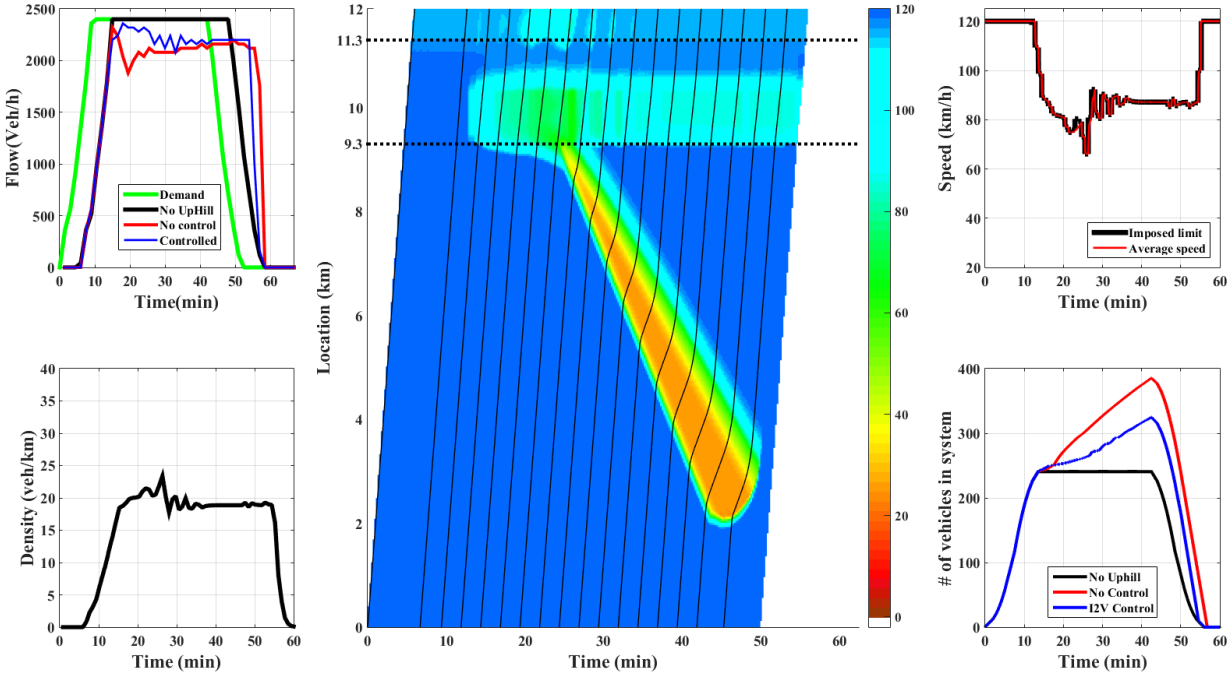

FIGURE 4 Input demand and exit flows (top left), density measured by loop detector (bottom left), heat-map with sample trajectories (middle), average vehicle speeds in the control section (top right), and number of vehicles in the system (bottom right) with a VSL control system at 100% CVs market penetration (delays are 49% lower than no control)

SENSITIVITY TO THE MARKET PENETRATION RATE

In this section, the market penetration level of the CVs is varied to understand the impacts on system performance. As arrivals of connected vehicles are assumed to be random, each market penetration level has been simulated 50 times to account for the variability. The results regarding reductions in total delays are presented as notched boxplots in Figure 5. First, as a percentage of CVs increases, the average improvement also increases but at a decreasing rate. Beyond a relatively small value of 15% market penetration, the average improvements are not substantially different from the maximum possible value of 49%. Second, there is substantial variation in the low market penetration rates, which rapidly diminishes with increasing CVs in the traffic stream.

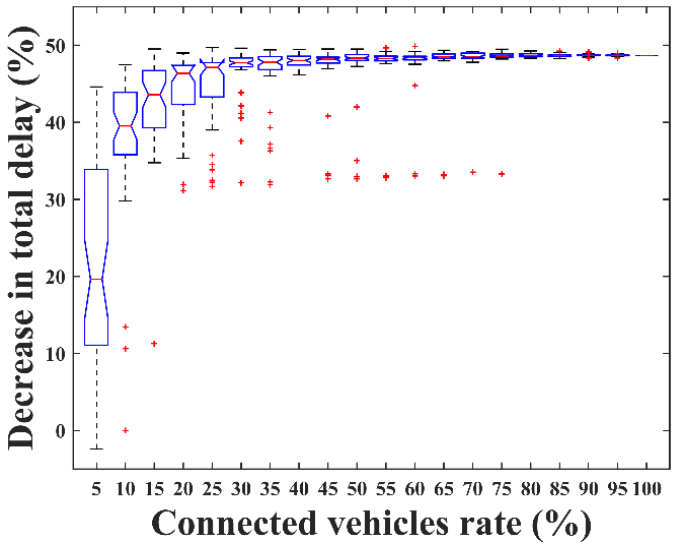

FIGURE 5 Notched boxplot of sensitivity analysis

Additional analyses are done to understand reasons behind the significant variations in the low market penetration levels. As it is shown in Figure 5, the highest variation is at the 5% penetration level which has improvements as high as 45%, or worse than the no control scenario. These two extreme cases are presented in Figure 6 and Figure 7 respectively. Each vertical red line added to the density diagrams (bottom left) indicates the exact time that a CV enters the control section. It is noticeable that the magnitude of improvement is correlated with the distribution of the arrivals of CVs over time. Whenever there is a large gap between the arrival of connected vehicles, density tends to rise with a delay.

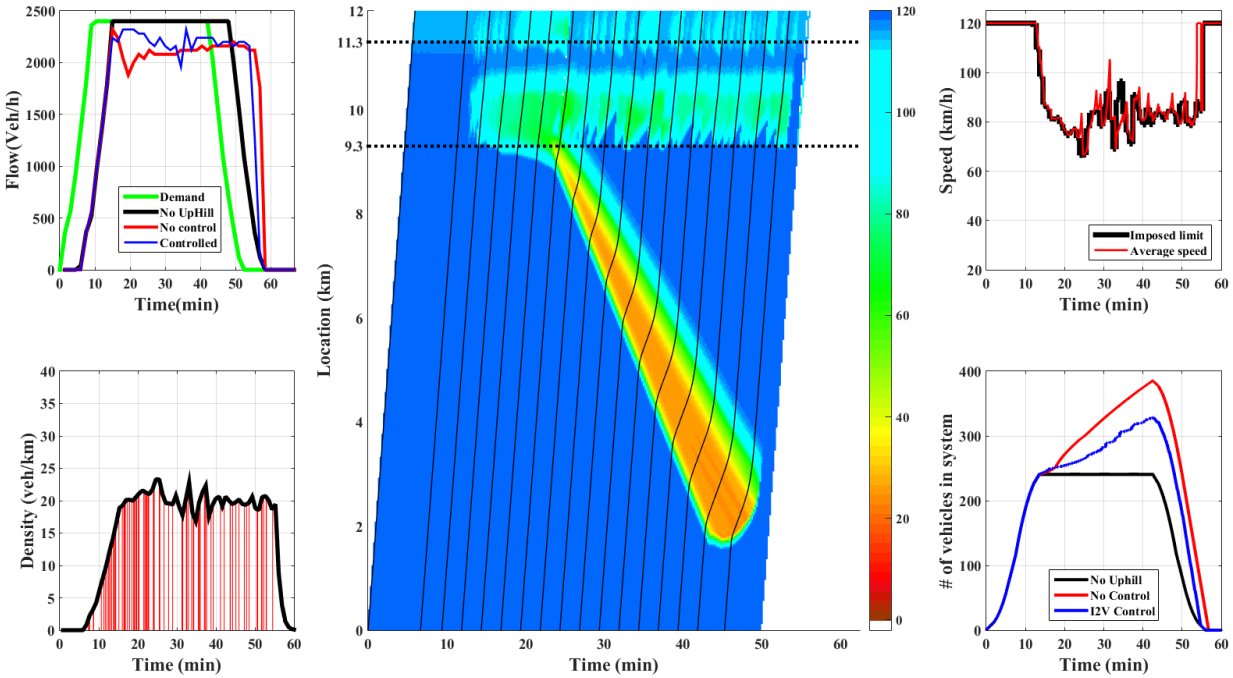

FIGURE 6 Same plots as in Figure 4 for a VSL control system with 5% CVs – a random scenario with good performance (delays are 44% better than no control)

The density diagram in Figure 3 (bottom left) shows how density at bottleneck would change if there is no control strategy. The most critical period for control strategy is between 15 to 25 minutes from the beginning of simulation which is the transition period from the uncongested to the congested traffic. After this period, congestion starts to propagate and grow backward. If the density of connected vehicles over time within this period is not enough to mitigate the initiation of the breakdown, the queue will extend from the bottleneck location (i.e., uphill) to the control sections. This will make a recovery to normal operations almost impossible. Density diagram (bottom left) of Figure 6 shows a denser arrival distribution around 15 to 25 minutes which kept density at bottleneck less than the critical point, and that is the main reason this sample has such a good performance. In contrary, the density diagram (bottom left) of Figure 7 has relatively huge gaps in the arrival of CVs around this period which leads to a significant spike in the density of bottleneck and clearly, the controller is not able to stabilize the system operation. This example illustrates the importance of the distribution of CVs within the traffic stream and how uneven or clustered arrivals can negatively impact system performance.

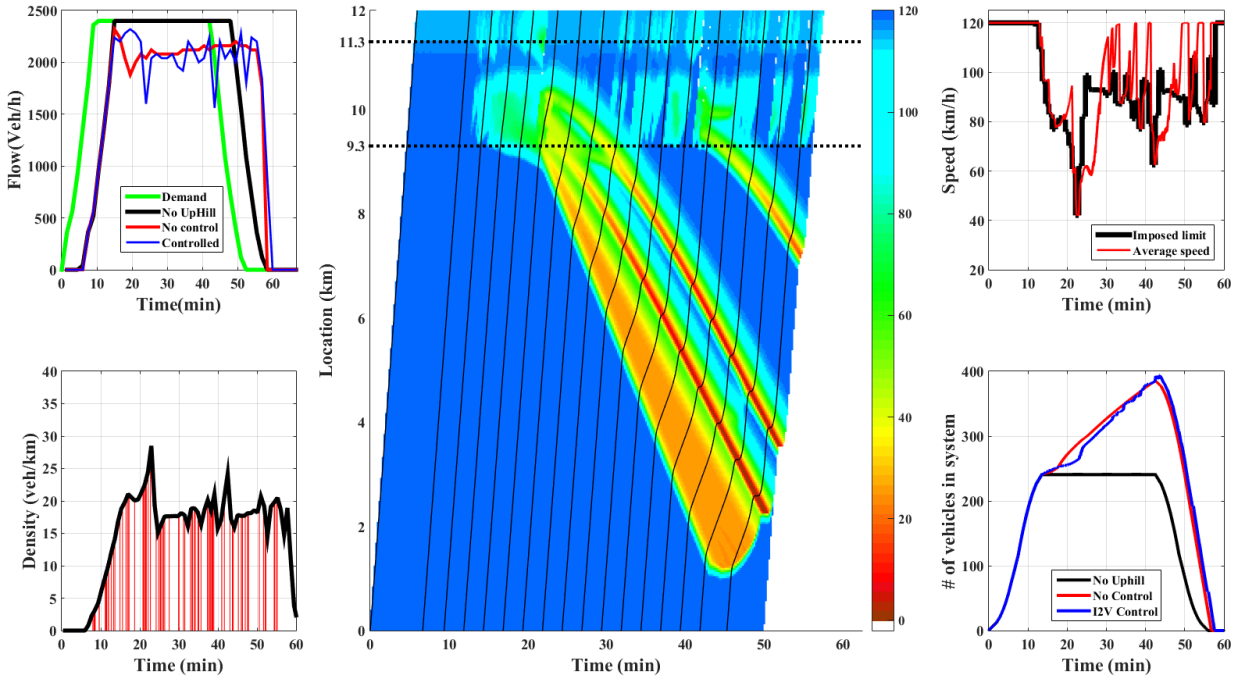

FIGURE 7 Same plots as in Figure 4 for a VSL control system with 5% CVs – a random scenario with bad performance (delays are 2% worse than no control)

CONCLUSION

In this paper, a VSL control strategy is developed to regulate the density of bottleneck on a sag curve. To improve system efficiency, connected vehicles (CVs) in the upstream control sections are instructed via V2I communications to adjust their speeds based on a VLS algorithm. The VSL prevents traffic from breaking down by using a proportional feedback control law. The optimal parameters are determined by a meta-heuristic algorithm called HPSOGA to get the best performance of the strategy. The results show that with optimal parameters for control strategy nearly half of the delay caused by the uphill can be eliminated. A sensitivity analysis shows that even with low market penetration rate (e.g., 15%) the system can reduce delays significantly. However, the control strategy is sensitive to the arrival times of CVs. If arrival times of CVs are not dense enough at the beginning of high demand, the performance of the system would drop considerably. It is demonstrated that measures of central tendency are not sufficient to understand the sensitivity of the system to market penetration rates of CVs due to large fluctuations in system performance, especially at 5-10% levels. For example, at 5% market penetration rate, the median improvement is 20% but the variance is so high that it includes negative performance as well as 45% improvement in total delays.

REFERENCES

1. Goni Ros, B., V. L. Knoop, B. Van Arem and S. P. Hoogendoorn. Car-Following Behavior at Sags and Its Impacts on Traffic Flow. *91st Annual Meeting Transportation Research Board, Washington, USA, 22-26 January 2012; Authors version*, 2012,

2. Ros, B., V. Knoop, B. van Arem and S. Hoogendoorn. Mainstream Traffic Flow Control at Sags. *Transportation Research Record: Journal of the Transportation Research Board*, No. 2470, 2014, pp. 57-64.

3. Papageorgiou, M., H. Hadj-Salem and F. Middelham. Alinea Local Ramp Metering: Summary of Field Results. *Transportation Research Record: Journal of the Transportation Research Board*, No. 1603, 1997, pp. 90-98.
4. Tilch, B. and D. Helbing. Evaluation of Single Vehicle Data in Dependence of the Vehicle-Type, Lane, and Site. In *Traffic and Granular Flow'99*, Springer, 2000.
5. Hall, F. L. and K. Agyemang-Duah. Freeway Capacity Drop and the Definition of Capacity. *Transportation research record*, No. 1320, 1991, pp.
6. Sohrabi, S., A. Ermagun and R. Ovaici. *Finding Optimum Capacity of Freeways Considering Stochastic Capacity Concept*. 2017.
7. Daganzo, C. and C. Daganzo *Fundamentals of Transportation and Traffic Operations*. Pergamon Oxford, 1997.
8. Manual, H. C. Transportation Research Board. *National Research Council, Washington, DC*, Vol. 113, 2000, pp.
9. Okamura, H., S. Watanabe and T. Watanabe. An Empirical Study on the Capacity of Bottlenecks on the Basic Suburban Expressway Sections in Japan. *Proceedings of the 4th International Symposium on Highway Capacity*, 2000, pp. 120-129.
10. Xing, J., K. Sagae and E. Muramatsu. Balance Lane Use of Traffic to Mitigate Motorway Traffic Congestion with Roadside Variable Message Signs. *Proceedings of ITS World Congress*, 2010,
11. Xing, J., E. Muramatsu and T. Harayama. Balance Lane Use with Vms to Mitigate Motorway Traffic Congestion. *International journal of intelligent transportation systems research*, Vol. 12, No. 1, 2014, pp. 26-35.
12. Furuichi, T., S. Yamamoto, M. Kotani and M. Iwasaki. Characteristics of Spatial Speed Change at Motorway Sag Sections and Capacity Bottlenecks. *82nd Annual Meeting of the Transportation Research Board, Washington, DC*, 2003, pp. 56-65.
13. Brilon, W. and A. Bressler. Traffic Flow on Freeway Upgrades. *Transportation Research Record: Journal of the Transportation Research Board*, No. 1883, 2004, pp. 112-121.
14. Yoshizawa, R., Y. Shiomi, N. Uno, K. Iida and M. Yamaguchi. Analysis of Car-Following Behavior on Sag and Curve Sections at Intercity Expressways with Driving Simulator. *International journal of intelligent transportation systems research*, Vol. 10, No. 2, 2012, pp. 56-65.
15. Laval, J. A. Effects of Geometric Design on Freeway Capacity: Impacts of Truck Lane Restrictions. *Transportation research part B: methodological*, Vol. 43, No. 6, 2009, pp. 720-728.
16. Koshi, M., M. Kuwahara and H. Akahane. Capacity of Sags and Tunnels on Japanese Motorways. *ite Journal*, Vol. 62, No. 5, 1992, pp. 17-22.
17. Komada, K., S. Masukura and T. Nagatani. Effect of Gravitational Force Upon Traffic Flow with Gradients. *Physica A: Statistical Mechanics and its Applications*, Vol. 388, No. 14, 2009, pp. 2880-2894.
18. YOKOTA, T. K. A Study of Ahs Effects on Traffic Flow at Bottlenecks. *TOWARDS THE NEW HORIZON TOGETHER. PROCEEDINGS OF THE 5TH WORLD CONGRESS ON INTELLIGENT TRANSPORT SYSTEMS, HELD 12-16 OCTOBER 1998, SEOUL, KOREA. PAPER NO. 3200*, 1998,
19. Oguchi, T. and R. Konuma. Comparative Study of Car-Following Models for Describing Breakdown Phenomena at Sags. *Proceedings of the 19th ITS World Congress*, 2009,
20. Treiber, M., A. Hennecke and D. Helbing. Congested Traffic States in Empirical Observations and Microscopic Simulations. *Physical review E*, Vol. 62, No. 2, 2000, pp. 1805.
21. Ozaki, H. Assistance of Drivers to Mitigate Highway Capacity Problem. *Steps Forward. Intelligent Transport Systems World Congress*, 1995,
22. Sato, H., J. Xing, S. Tanaka and T. Watauchi. An Automatic Traffic Congestion Mitigation System by Providing Real Time Information on Head of Queue. *16th ITS World Congress and Exhibition on Intelligent Transport Systems and Services*, 2009,
23. Cetin, M., P. Foytik, S. Son, A. J. Khattak, R. M. Robinson and J. Lee. *Calibration of Volume-Delay Functions for Traffic Assignment in Travel Demand Models*. 2012.
24. Li, K., L. Kang, W. Zhang and B. Li. Comparative Analysis of Genetic Algorithm and Ant Colony Algorithm on Solving Traveling Salesman Problem. *Semantic Computing and Systems, 2008. WSCS'08. IEEE International Workshop on*, 2008, pp. 72-75.
25. Bai, Q. Analysis of Particle Swarm Optimization Algorithm. *Computer and information science*, Vol. 3, No. 1, 2010, pp. 180.
26. Duan, H., Q. Luo, Y. Shi and G. Ma. Hybrid Particle Swarm Optimization and Genetic Algorithm for Multi-Uav Formation Reconfiguration. *IEEE Computational intelligence magazine*, Vol. 8, No. 3, 2013, pp. 16-27.

27. Papageorgiou, M., C. Diakaki, V. Dinopoulou, A. Kotsialos and Y. Wang. Review of Road Traffic Control Strategies. *Proceedings of the IEEE*, Vol. 91, No. 12, 2003, pp. 2043-2067.